

## General Disclaimer

### One or more of the Following Statements may affect this Document

- This document has been reproduced from the best copy furnished by the organizational source. It is being released in the interest of making available as much information as possible.
- This document may contain data, which exceeds the sheet parameters. It was furnished in this condition by the organizational source and is the best copy available.
- This document may contain tone-on-tone or color graphs, charts and/or pictures, which have been reproduced in black and white.
- This document is paginated as submitted by the original source.
- Portions of this document are not fully legible due to the historical nature of some of the material. However, it is the best reproduction available from the original submission.

DUAL EXPOSURE INTERFEROMETRY

G. Smeets and A. George



Translation of "Doppelbelichtungs-Interferometrie",  
Institut Franco-Allemand de Recherches, St. Louis  
(France) Report ISL-39-72, 4 Dec. 1972, pp. 1-22.

(NASA-TM-77002) DUAL EXPOSURE  
INTERFEROMETRY (National Aeronautics and  
Space Administration) 20 p HC A02/MF A01

N83-21262

CSCS 20D

Unclass

G3/34 09333

STANDARD TITLE PAGE

1. Report No. NASA TM 77002		2. Government Accession No.		3. Recipient's Catalog No.	
4. Title and Subtitle DUAL EXPOSURE INTERFEROMETRY				5. Report Date December 1982	
				6. Performing Organization Code	
7. Author(s) G. Smeets and A. George				8. Performing Organization Report No.	
				10. Work Unit No.	
9. Performing Organization Name and Address SCITRAN Box 5456 Santa Barbara, CA 9310A				11. Contract or Grant No. NASw 3542	
				13. Type of Report and Period Covered Translation	
12. Sponsoring Agency Name and Address National Aeronautics and Space Administration Washington, D.C. 20546				14. Sponsoring Agency Code	
				15. Supplementary Notes  Translation of "Doppelbelichtungs-Interferometrie", Institut Franco-Allemand de Recherches, St. Louis (France) Report ISL-39-72, 4 Dec. 1972, pp. 1-22. (N74-10459)	
16. Abstract  The application of dual exposure differential interferometry to gas dynamics and flow visualization is discussed. A differential interferometer with Wallaston prisms can produce two complementary interference fringe systems, depending on the polarization of the incident light. If these two systems are superimposed on a film, with one exposure during a phenomenon, the other before or after, the phenomenon will appear on a uniform background. By regulating the interferometer to infinite fringe distance, a resolution limit of approximately $\lambda/500$ can be obtained in the quantitative analysis of weak phase objects. This method was successfully applied to gas dynamic investigations.					
17. Key Words (Selected by Author(s))			18. Distribution Statement  Unclassified - Unlimited		
19. Security Classif. (of this report) Unclassified		20. Security Classif. (of this page) Unclassified		21. No. of Pages 20	22. Price

DUAL EXPOSURE INTERFEROMETRY

G. Smeets and A. George\*

Summary

\*\*/3

A differential interferometer with Wollaston prisms can produce two complementary interference fringe systems, depending on polarization direction of the incident light. If both systems are superimposed on a film, by carrying out one exposure during the process and carrying out the other exposure either before or afterwards, then the process seems to appear on a uniform background. By adjusting the interferometer to infinite fringe separation, during the quantitative evaluation of weak phase objects, one can achieve a resolution limit of about  $\lambda/500$ . The method was used successfully for gas dynamic investigations.

Key words

/4

double exposure interferometry  
polarized light  
differential interferometry  
gas dynamics  
interferometers  
experiments  
measurement methods  
fluid mechanics  
optics

---

\* ISL Report 39/72, French-German Research Institute, St. Louis, France, December 1972.

\*\*Numbers in margin indicate pagination of foreign text.

Table of Contents

**ORIGINAL PAGE IS  
OF POOR QUALITY**

75

	<u>page</u>
Introduction	5
Double exposure with complementary interferences	3
Optical configurations	5
Interferograms of weak phase objects	6
Quantitative evaluation of the interferograms	7
Interferograms of strong phase objects--double exposure Schlieren systems	9
Visualization of motions	10
References	12
Figures	12

Introduction

Phase objects are made visible on interferograms by means of a displacement of the interference fringes. Figure 1 shows the limiting case of a very weak phase object where the resulting fringe displacement is only about 1/20 of the fringe separation and can hardly be distinguished (top figure in Figure 1). Here we are considering a sequence of pressure waves which emerge from a small opening in a capsule after a spark discharge has taken place inside the capsule.

The weak phase object becomes better visible when the interferometer is adjusted to infinite fringe separation and average brightness (lower left figure). In this way, the sensitivity can be substantially increased. The spot background of the image occurs because of small errors in the optical components in the interferometer and first is unavoidable because small residual errors always occur in the most complex optics.

By means of a double exposure of the film with two complementary interference systems (that is, also complementary spots), one can bring about a uniform image background. When the first exposure is done beforehand, and the second in the presence of the phase object, then the object will appear against an undisturbed background. In this way, a quantitative densitometric evaluation is possible. Using higher contrast film, the sensitivity can be increased further so that optical path changes of  $\lambda/500$  can be resolved.

Double exposure using complementary interferences

An ideal two-beam interferometer produces a modulation with the illumination intensity

$$E = E_0 \cos^2 \left\{ \pi \frac{\Delta\phi}{\lambda} \right\}, \quad (1)$$

in the image plane where  $\lambda$  is the light wavelength and  $\Delta\phi$  is the optical path difference of a light beam pair which experiences

interference at a given image point. If the interferometer is adjusted to infinite fringe separation, then this means that  $\Delta\phi$  is made the same for all image points. Because of the optical errors, one cannot avoid that  $\Delta\phi$  varies in the image plane over a certain interval and spots are produced. Using good optical components, the interval, however, can be made so small that it lies entirely on a straight line central part of an interference edge (Figure 2). In 8 this case, small changes in the optical path difference due to a phase object  $d\Delta\phi$  are converted to changes in the illumination intensity  $dE$  at the corresponding image point which are proportional and the proportionality factor remains the same over the entire image. From equation (1) we find the following for small optical path difference changes along the edge:

$$(2) \quad dE = \frac{\pi \cdot E_c}{\lambda} \sin \left\{ 2\pi \frac{\Delta\phi}{\lambda} \right\} \cdot d\Delta\phi = \frac{\pi \cdot E_0}{\lambda} d\Delta\phi .$$

In order to compensate for the spots due to optical errors, the film is exposed twice. One of the exposures is performed in the presence of the phase object. The illumination intensity is here given by the sum  $E + dE$  of equations (1) and (2). The second exposure for compensating the errors can occur before or after the process and has to have the interference modulation which is complementary to that given by equation (1):

$$(3) \quad \bar{E} = E_c \cdot \sin^2 \left\{ \pi \frac{\Delta\phi}{\lambda} \right\} .$$

For the same exposure time of the two partial exposures, the film is given a total exposure which is proportional to the sum of the illumination intensities:

$$(4) \quad E + dE + \bar{E} = E_0 \left( 1 + \pi \frac{d\Delta\phi}{\lambda} \right) .$$

This only depends on  $d\Delta\phi$  in a linear manner and no longer on  $\Delta\phi$ ; i.e., the phase object seems to appear against a uniform background. By densitometric determination of the illumination, according

**ORIGINAL PAGE IS  
OF POOR QUALITY**

to equation (4), the optical path change in the phase object  $d\Delta\phi$  can be determined quantitatively.

A small optical path change  $d\Delta\phi$  leads to a blackness change as follows on the film:

$$(5) \quad dS = S - S_0 = 0.434 \gamma \cdot \frac{d\Delta\phi}{\lambda} .$$

It is assumed that the exposure leads to the straight part of the blackness curve with the inclination  $\gamma$ .

A good densitometer can resolve blackness changes of  $dS = 1/100$  so that high contrast films ( $\gamma=4$ ) can bring about a resolution limit for optical path changes of  $d\Delta\phi = \lambda/500$ .

Equations (1) to (9) are set up for monochromatic light for 9 simplicity. The compensation can be carried out just like for white light if the two interference components for each wavelength have a complementary behavior according to equations (1) and (3). All of the examples shown were photographed with sparks or tube flash equipment which give off white and not coherent light.

### Optical configurations

It is possible to realize the method in a simple manner using a differential interferometer with a Wollaston prism. Such an interferometer operates with polarized light. In the case of linear polarization, the two polarization directions lead to complementary interferences.

By using an additional Wollaston prism, it is possible to focus two independent spark and flash light sources on the inlet diaphragm of the differential interferometer (Figure 3). The two light bundles which enter the interferometer coincide and are polarized normal to one another and consequently lead to complementary interferences.



**ORIGINAL PAGE IS  
OF POOR QUALITY**

The differential interferometer itself consists of a pair of Wollaston prisms, a pair of objectives (or a pair of concave mirrors in the usual Z configuration), an additional polarization filter and a camera which maps the phase object in the test chamber on to the screen or the film. Additional details of the interferometer are given in [1,2,3].

For the compensation method, it is very important that the differential interferometer has a small sensitivity to vibrations. The adjustment of the interferometer to the central straight line part of the interference edge must be maintained and cannot be disturbed by small tremors.

Figure 4 gives the ray path for a single light source with multiple flashes. The light source is enlarged and mapped on to a Pockels cell. Between the two exposures, the Pockel cell is switched with the  $\lambda/2$  voltage and in this way, the polarization of the light is rotated by  $90^\circ$ . With the circuit of the Pockel cell, interference fringes are displaced and the absolute value of the fringe displacement is the same for all wavelengths. Therefore, the fringe system is displaced as a whole and undistorted even for white light. /16

When switching with the  $\lambda/2$  voltage (of an average wavelength), the fringes are displaced so much that the central part of the positive edge to the left of the central fringe of zero order is displaced into the central part of the negative edge on the other side.

Interferograms of weak phase objects

Figure 5 shows two double exposure interferograms of hypersonic flows of small density around blunt cones. The density of the incident flow in the left figure was  $1.2 \cdot 10^{-3} \rho_0$  and in the right figure, it was  $3.2 \cdot 10^{-3} \rho_0$ . The Mach number in both cases was about 9. The nose radii were 20 mm and 10 mm, respectively.

The limiting case of a very weak phase object which only produces an optical path change of about  $\lambda/500$  and can just be made

**ORIGINAL PAGE IS  
OF POOR QUALITY**

visible is given in Figure 6. The nose radius here has a diameter of 5 mm and the incident flow density is only  $7 \cdot 10^{-4} \rho_0$ .

All three figures were recorded on the agfa L AGEPEFF emulsion. This photograph material has some properties which are advantageous for double illumination interferometry. In addition to good resolution capacity, there is high contrast ( $\gamma=4$ ). However, this emulsion has a specially small Schwarzschild effect. In the case of deviations from the photographic reciprocal law, no complete compensation can be achieved.

Xenon flash tubes are used as light sources whose illumination time were adjusted to about 50  $\mu$ s. We intentionally selected a rather long exposure time. This is favorable from the point of view of the Schwarzschild effect. Also, in this way the turbulences ahead of the test section windows can be made invisible because they move away fast. The flow around the model remains stationary during the exposure time.

The very high contrast photographs place extreme cleanliness requirements on the test section window. An absorption of only 1% for a contrast factor of  $\gamma = 4$  is already visible on the film as a perturbation, and the windows will still look clean upon direct observation. Also, any small damages to the windows by membrane fragments appear very large.

/11

Quantitative evaluation of interferograms

The phase objects appear in front of a uniform background without perturbations on double exposure interferograms and, therefore, they can be quantitatively measured. This is done in two steps. First of all, for each individual point the optical path changes in the phase object  $d\Delta\Phi$  are determined. From this, in the case of two-dimensional or rotationally symmetric objects, it is possible to determine their index of refraction distribution. Here we will only

**ORIGINAL PAGE IS  
OF POOR QUALITY**

discuss the first step. The second step is discussed in detail in [3] and is a generally valid principle for the evaluation of differential interferograms.

When recording interferograms, one has to make sure that all image points remain along the straight part of the interference edge and that the exposure of the film is in the region of constant inclination of the blackness curve everywhere. Then on the one hand, we have the relationship

$$I = I_0 \left( 1 + \pi \frac{d\Delta\phi}{\lambda} \right) \quad (6)$$

between the exposure  $I$  and the optical path change  $d\Delta\phi$ . Also, there is a simple relationship between blackness and illumination:

$$S = S_0 \cdot \gamma \lg I/I_0. \quad (7)$$

The combination of both equations finally gives a relationship between the blackening changes determined densitometrically on the film  $dS$  and the optical path changes  $d\Delta\phi$ :

$$d\Delta\phi = \frac{\lambda}{\pi} \left( \exp \left\{ \frac{dS}{0.4343 \cdot \gamma} \right\} - 1 \right). \quad (8)$$

The evaluation using this equation also requires the exact knowledge of the average path length  $\lambda$  and the contrast factor  $\gamma$ .  $\lambda$  is only a measure for the inclination of the interference edge and can be determined before hand using interferences with monochromatic light.  $\gamma$  on the other hand, depends on many conditions, for example, the developer and development time and, therefore, experiences fluctuations. It is appropriate to determine  $\gamma$  with calibration. There are many possibilities for this. For each photograph one could also photograph a weak neutral filter with an exactly known attenuation. In the case of differential interferograms, there is a much simpler possibility. The interferograms have a double image. The edge regions where the two partial images do not overlap do not contain any interferences. It is easy to show that here the exposure is exactly one-half of the exposure of the uniform image background

**ORIGINAL PAGE IS  
OF POOR QUALITY**

outside of the phase object. By measuring the corresponding blackening difference, it is possible to determine the factor  $\gamma$  of the photograph using equation (7). One condition, of course, is that the edge regions mentioned also are in the range of constant inclination of the blackening curves. /12

Interferograms of stronger phase objects--double exposure Schlieren system

The double illumination interferometry was originally developed in order to be able to obtain interferograms of weak phase objects which could be evaluated. The method in a modified form can also be used for stronger phase objects, and the most important advantages are maintained. The optical path changes have to be restricted to about  $\lambda/10$  so that they remain on the selected interference edge. This can be achieved in the case of the differential interferometer by selecting a correspondingly small ray separation  $a$ . In this way, the interferometer becomes sensitive to gradients, that is, the measured optical path changes  $d\Delta\phi$  are given by gradients:

$$(9) \quad d\Delta\phi = a \cdot \text{grad } \phi = a \int \text{grad } n \, ds .$$

The quantitative evaluation is exactly the same as for a Schlieren photograph and gives the gradient field of the phase object. There are the following advantages compared with the Schlieren method:

1. The optics do not have to be of exceptional quality in order to give photographs which can be quantitatively evaluated with a uniform image background.

2. The radiation path can be very sensitive without becoming low intensity at the same time, as cannot be avoided in the case of the Schlieren method.

3. The relationship between the exposure and  $\text{grad } \phi$  is direct and is not influenced by refraction effects as is the case for the sensitive Schlieren method.

**ORIGINAL PAGE IS  
OF POOR QUALITY**

The sensitivity of the method can be varied over a wide range by selecting a and can, therefore, always be matched to the phase objects in an optimum way. For very strong phase objects, a would have to be made very small in order to not oversteer the interferometer. In this case, it is more appropriate to use a Schlieren method with a correspondingly low sensitivity which will not have the disadvantages mentioned under 2 and 3 above. If there is a small sensitivity, also a double exposure Schlieren system can be designed which allows error compensation and gives images which can be evaluated even for very simple optics. The ray path is shown in Figure 13 7. Just like in Figure 3, two independent light sources are focused using a Wollaston prism onto the inlet slit of the Schlieren device. The incoming light bundles are polarized perpendicular to one another. By using a second Wollaston prism, a double image of the inlet slit is produced at the position of the Schlieren edge. Instead of the Schlieren edge, there is a second slit there which acts as a double Schlieren edge. By appropriately setting the position and width of this slit, one can produce two complementary Schlieren images inside one another for the two polarization directions. The third Wollaston prism is required in order to reverse the splitting of the image in the second prism so that both Schlieren images cover exactly on the film or on the screen.

Visualization of motions

Double image interferometry leads to another effect if both exposures are carried out when the phase object is present. In addition to disturbances by flaws in the optics, the phase object itself is suppressed to the extent that it is stationary. All changes which occur during the time interval between the two exposures then emerge clearly. By suitable tuning of the illumination time and the time interval between the exposures, it is possible to make visible certain motions and the faster motions can be smeared by sufficiently long exposure time. On the other hand, the slow motions can be suppressed by the double exposure if the time interval is not too large.

**ORIGINAL PAGE IS  
OF POOR QUALITY**

Figure 8 shows a turbulent airstream produced by a small ventilator. The airstream is best visible where its speed is the largest. The relatively slow secondary flow in the outer regions is completely invisible. For direct observation of the screen, the reverse is true. The eye cannot perceive the rapidly moving turbulent airstream, but it only sees the outer stream.

One interesting application of separating fast motions from slow motions is the sound radiation of gas dynamic objects. The acoustic waves which are formed represent a rapidly moving weak phase object which in many cases is superimposed by stronger phase objects, but they move much slower. In this application, the high sensitivity is very important because the acoustic waves in general represent very weak phase objects. /14

Figures 9 and 10 give examples of ultrasonic waves of frequency 22 kHz, which are radiated by a rod in the airstream. Figure 10 shows the waves of a flat plate made of Styropor.

Figures 11 and 12 give the supersonic free jet at the end of a shock tube which has completely different appearances in both figures. Figure 11 was taken with two 60- $\mu$ s exposures and the first exposure was made before the free jet was created. Figure 12, on the other hand, was taken with two 1- $\mu$ s exposures which both were carried out when the free jet was present and at a time separation of 10  $\mu$ s. In this way, the stationary structures of the free jet are for the most part suppressed and the radiated acoustic waves as well as the individual turbulence balls appear clearly. There are two weak reflected shockwaves on the upper and lower edge of the image which can be seen which run against the free jet.

ORIGINAL PAGE IS  
OF POOR QUALITY

References

/14

- [1] H. Oertel. A differential interferometer for measuring hypersonic shock tubes. ISL-T 17/61 (1961).
- [2] G. Smeets. Differential interferometer for observing and measuring boundary layers. ISL-T 25/04 (1964).
- [3] G. Smeets. Differential interferometer with large bundle separation. Evaluation of interferograms. ISL - T 41/68 (1968).

/1

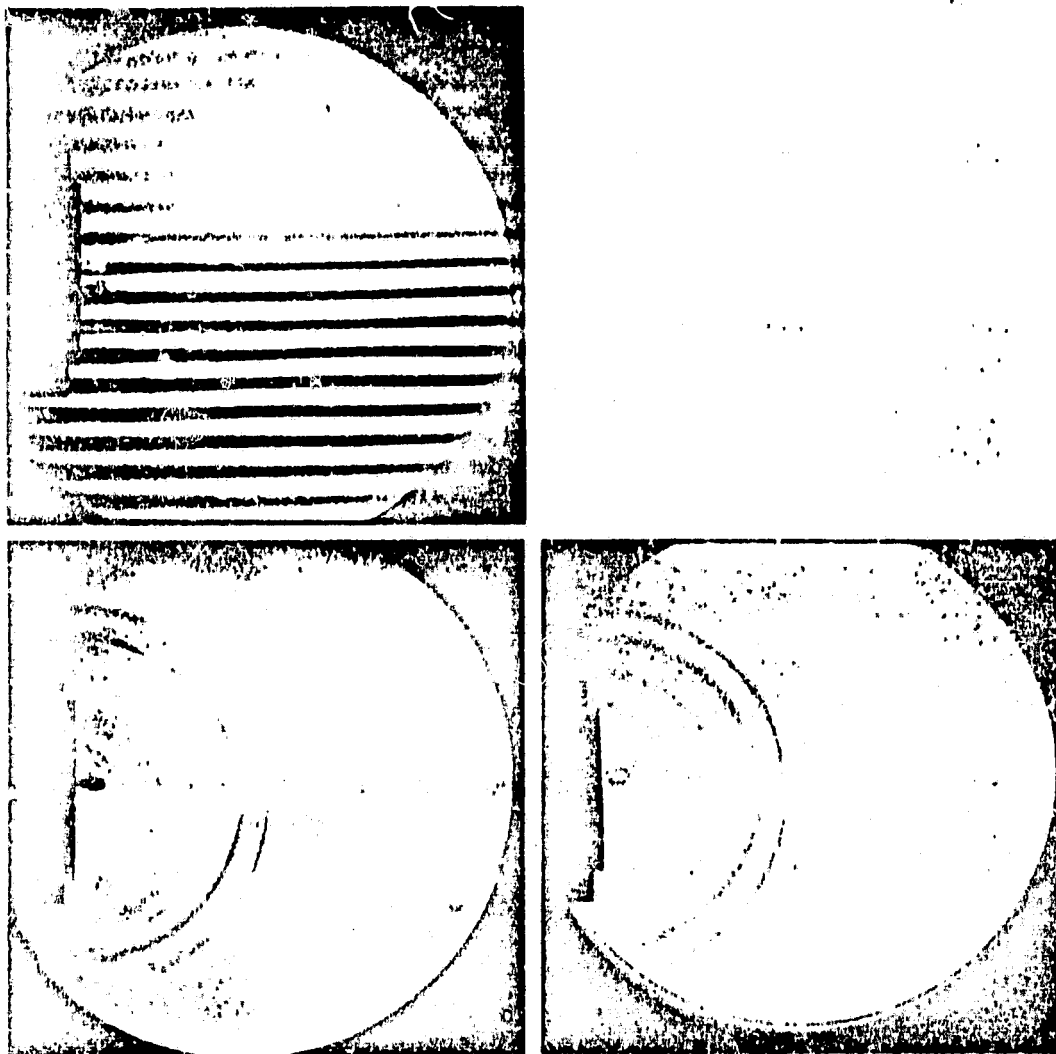


Figure 1

ORIGINAL PAGE IS  
OF POOR QUALITY

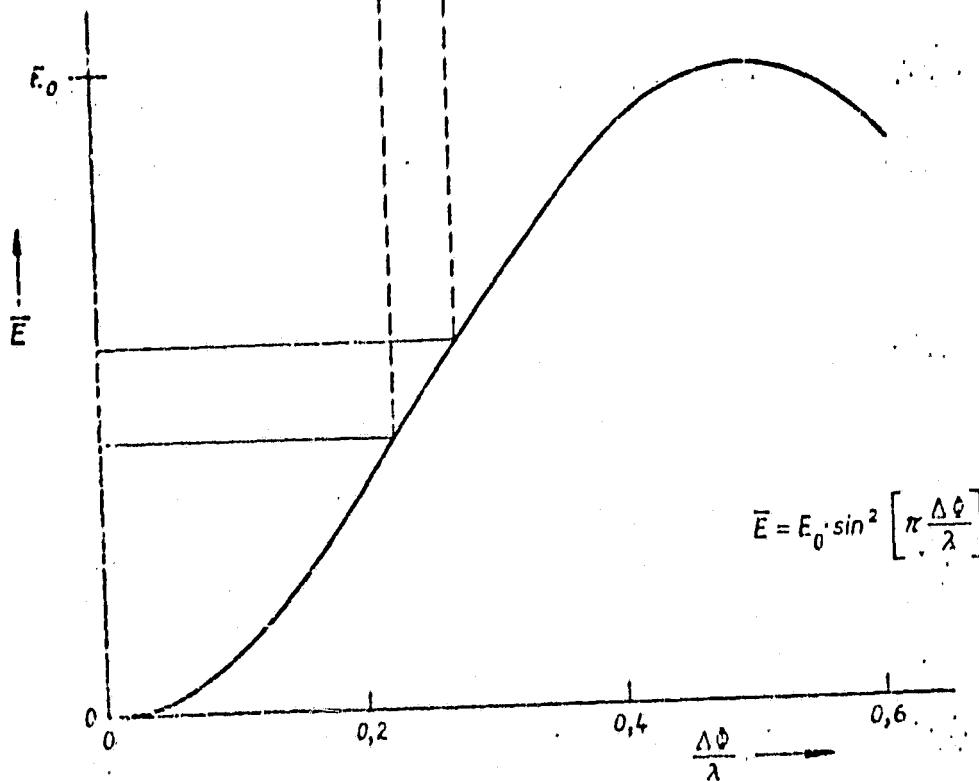
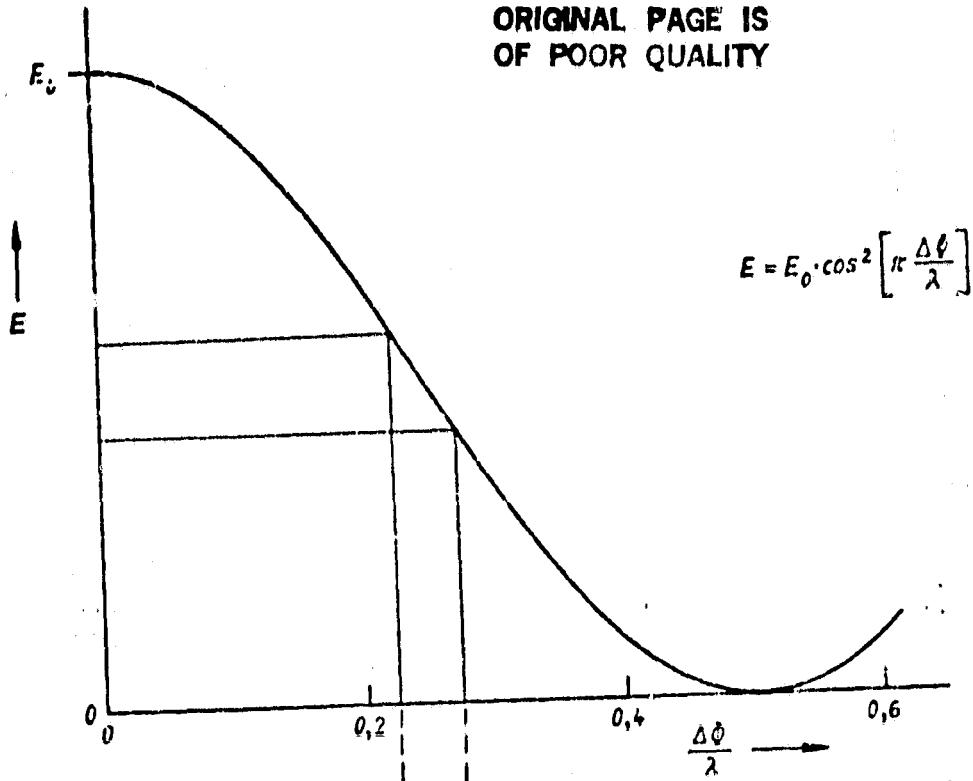


Fig. 2



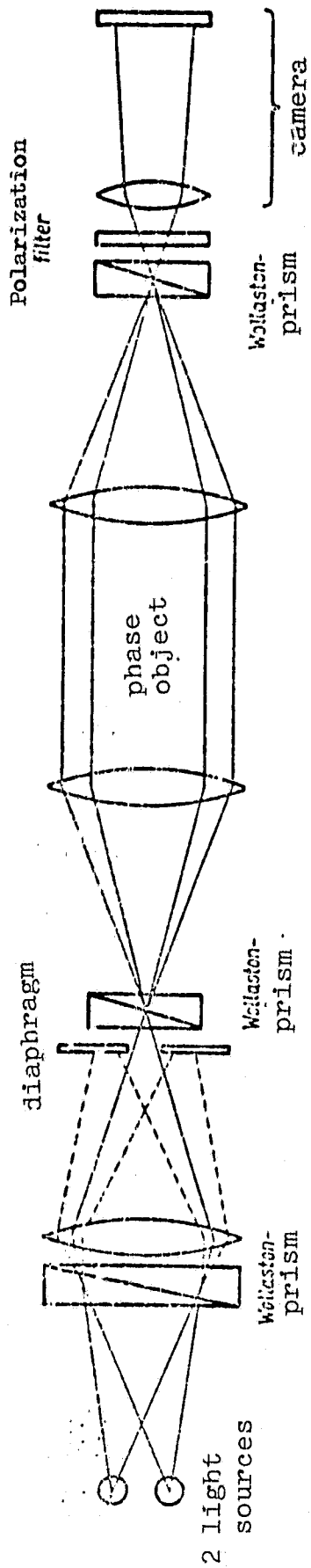


Figure 3

ORIGINAL PAGE IS  
OF POOR QUALITY

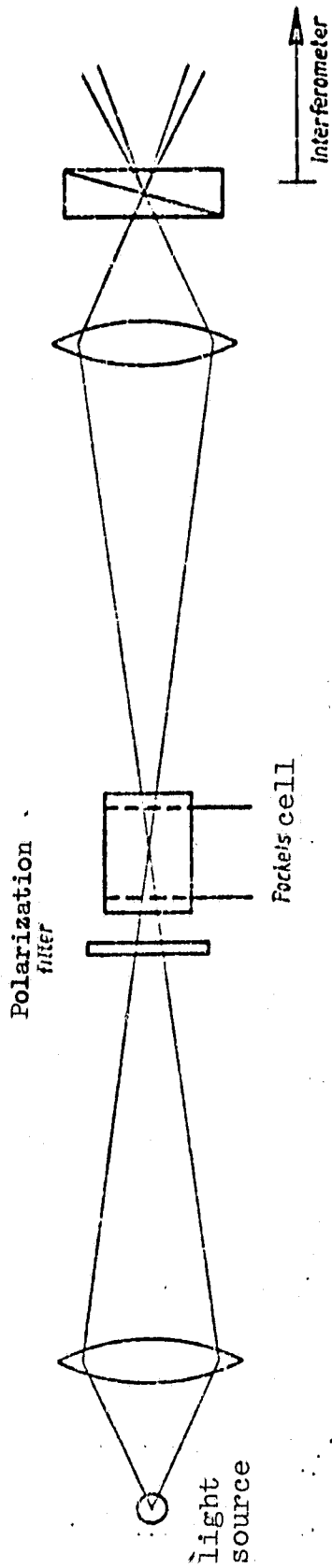


Figure 4

ORIGINAL PAGE IS  
OF POOR QUALITY

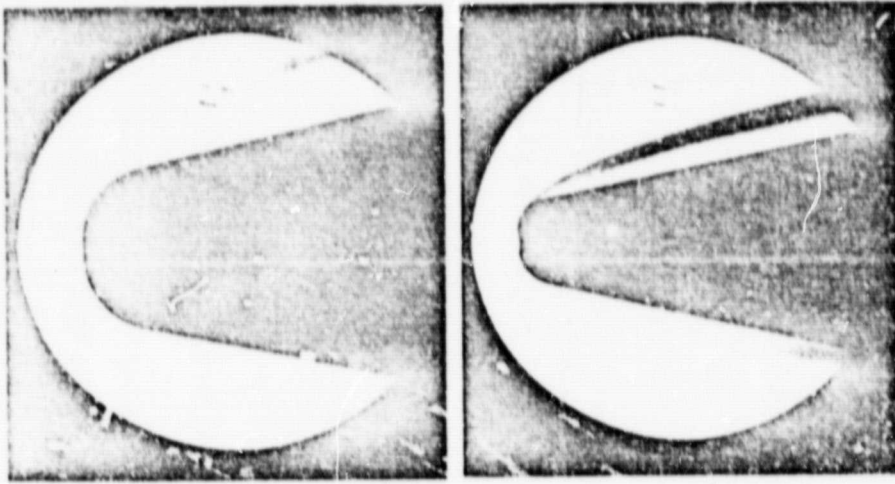


Figure 5

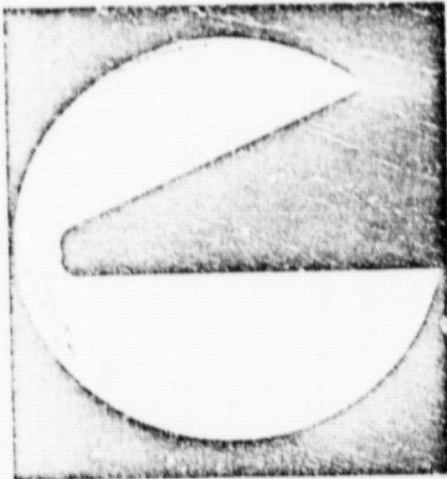


Figure 6

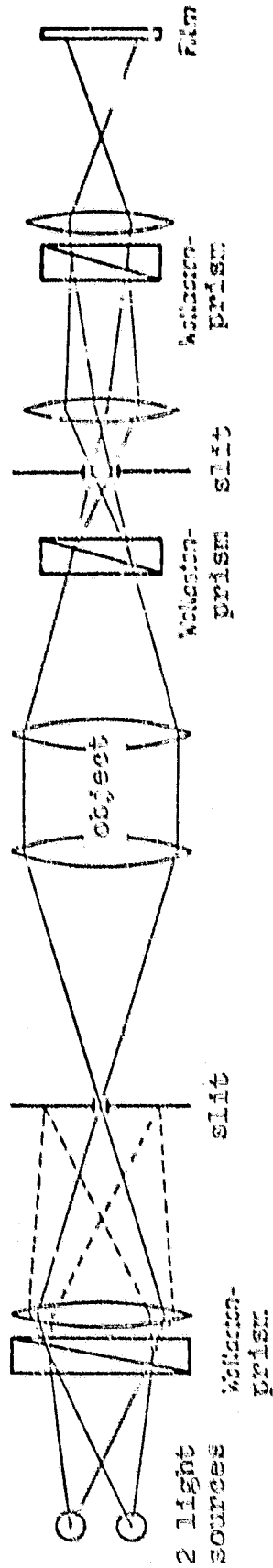
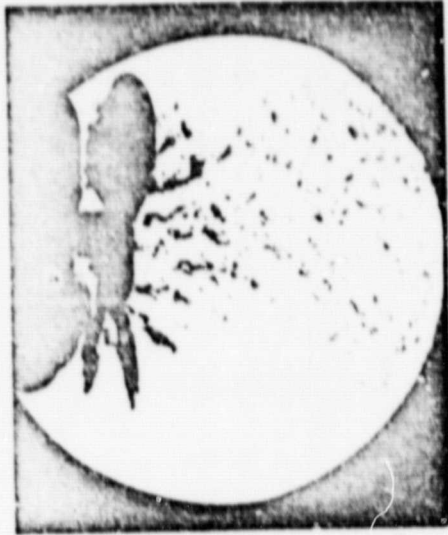


Figure 7



ORIGINAL PAGE IS  
OF POOR QUALITY

Figure 8

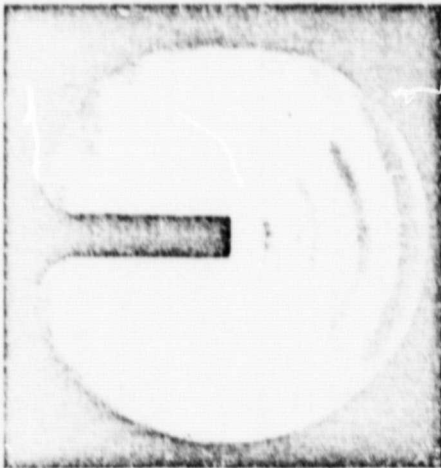


Figure 9

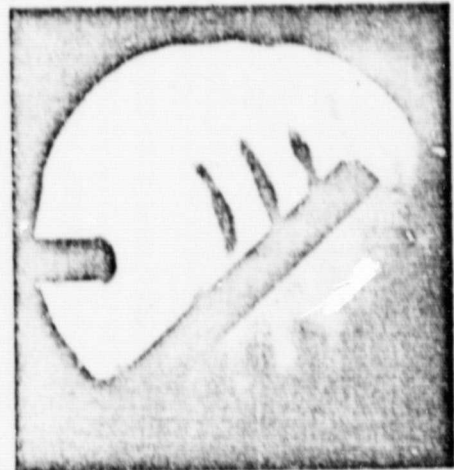


Figure 10

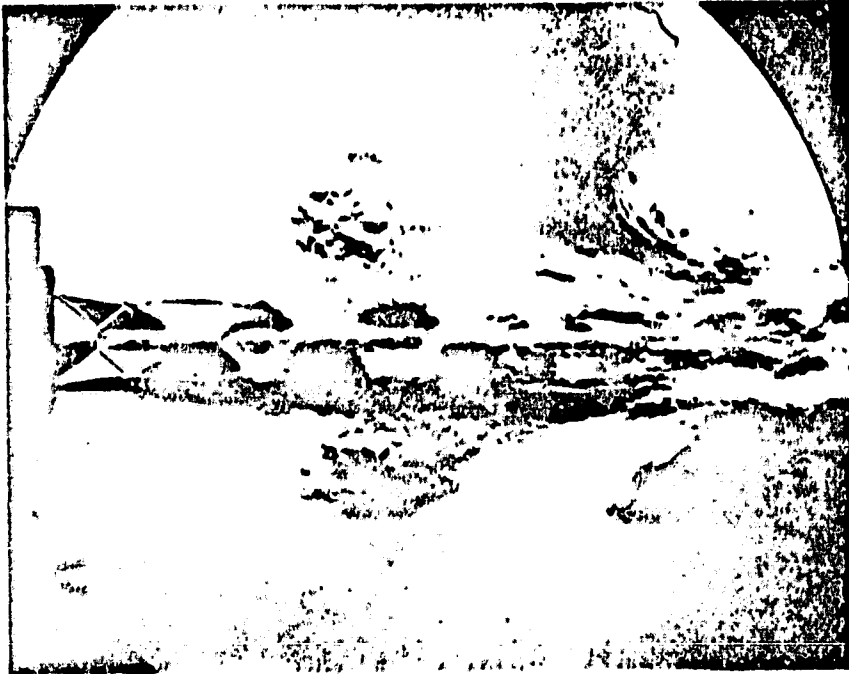


Figure 11



Figure 12